JOURNAL OF THEORETICAL AND APPLIED MECHANICS
48, 3, pp. 715-731, Warsaw 2010

STUDY OPERATION OF THE ACTIVE SUSPENSION SYSTEM OF A HEAVY MACHINE CAB

Grzegorz Tora

Cracow University of Technology, Institute of Machine Design, Kraków, Poland
e-mail: tora@mech.pk.edu.pl

This study is a part of research on active suspension systems of cabs in heavy machines and trucks, used for suppressing low-frequency and large-amplitude vibrations. The suspension system incorporates two platform mechanisms placed one upon the other. The lower mechanism is responsible for maintaining the cab in the vertical position whilst the upper mechanism controls the cab movements in the vertical direction. Motion of the cab is described using versors associated with the mechanism links. Relationships are derived that yield the instantaneous velocities of the drives that lead to reduction of the cab vibrations in selected DOFs. The procedure is shown for calculating the loads acting on the drives of the active suspension during the specified movement of the machine frame. The mathematical model is further utilised in simulations of the suspension operation.

Key words: active vibration reduction, cab suspension, platform mechanism

1. Introduction

When heavy machines and tractors move in rough terrain, vibrations of the operator cab are generated in its certain DOFs. After a while, high-amplitude vibrations (up to 0.5 m in the vertical direction) of low frequency (up to 5 Hz) make the machine operator tired and less efficient whilst the work safety features tend to deteriorate. In order to improve the operator's comfort while at work, an active suspension of the cab can be incorporated in the machine structure. Such an active suspension system incorporates an actuator mechanism that handles the drives and the energy sources, the system measuring the machine vibrations and the control system. The measurement system is responsible for collecting real-time information about the movements of the

machine frame and the drives (Cardou and Angeles, 2008). The computer uses this information to derive instantaneous velocities of hydraulic drives which shall induce the movements of the actuator mechanism placed between the frame and the cab to reduce low-frequency vibrations of the cab in selected DOFs.

Active vibration reduction systems were first introduced in the suspensions of the operator's seats, they were then incorporated in the mounts of the driver's cabs in trucks, tractors and heavy machines. Typically, effective vibration control of the driver's seat can be achieved in the vertical direction only. Passive, semiactive and active solutions in the suspensions of farming tractors and trucks normally involve a greater number of DOFs, whilst the amplitudes of motion are relatively small (Nakano *et al.*, 1999). The active suspension of a cab with two degrees of mobility is applied in heavy trucks used in forestry. Cab displacements (especially lateral displacements) in heavy trucks, where they are positioned relatively high, are considerable while the machine travels in rough terrain. Therefore, the author proposes a structure of the actuator mechanism that would fully answer the case (Tora, 2008).

2. Structure of the mechanism

The structure of the mechanism and the number of drives are decided arbitrarily, depending on the number of DOFs to be handled. While a heavy truck moves in rough terrain, the largest vibrations of a high-positioned cab are registered along the lateral axis of the machine y_r, along the vertical axis z and around the axes x_r and y_r. Vibration reduction around the z_r-axis seems unnecessary as they prove negligible during the ride. When veering, the cab should rotate with the machine frame. For simplicity, vibrations along the x_r-axis are neglected, too (Fig. 1).

The active suspension mechanism incorporates two platform mechanisms stacked serially one upon the other. The lower mechanism (see Fig. 2) ought to, inter alia, maintain the cab in the direction of the gravity force. The lower mechanism consists of platform 6 suspended on boards 2 and 3 with the use of spherical pairs D and E. Boards 2 and 3 are connected to machine frame 1 by revolving pairs. Along the section DE, machine frame 1, boards 2 and 3, and platform 6 form a planar mechanism working in the plane $y_r z_r$ and set in motion by cylinder 4. Cylinder 5, connected to platform 6 and frame 1 by spherical pairs A and G, induces rotating motion of platform 6 around the direction defined by points D and E. The mechanisms presented above

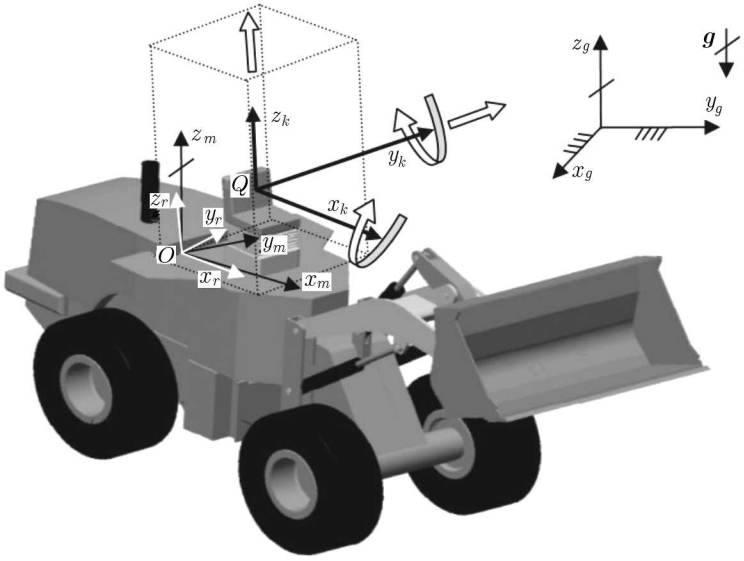

Fig. 1. Coordinate system. DOFs to be handled by the vibration reduction system

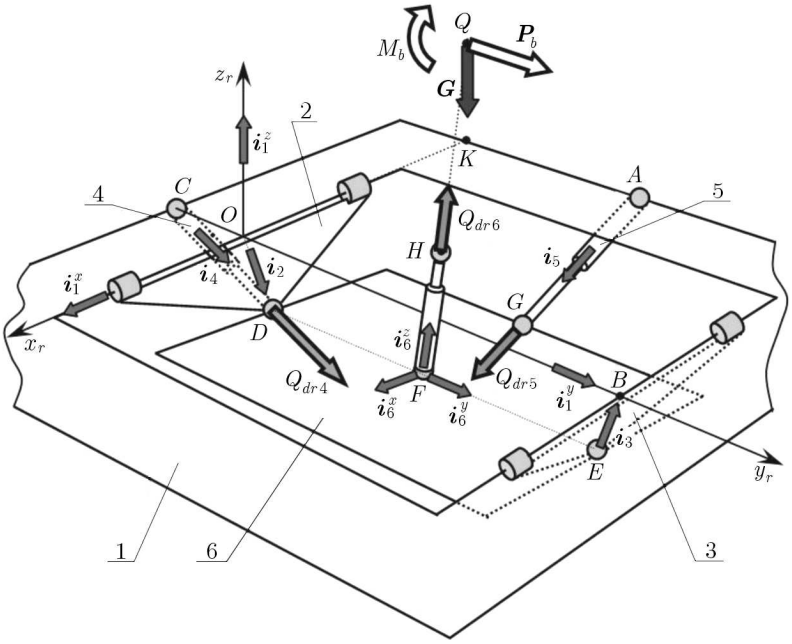

Fig. 2. Lower platform mechanism maintaining the cab in the vertical position, link versors, systems of driving forces, inertia and gravity forces

has 2 degrees of mobility. The dimensions l_{OD}, l_{DE}, l_{BE}, l_{OB} can be chosen such that one cylinder 4 should suffice to reduce the vibrations of platform 6 in 2 DOFs (rotation around the x_r-axis and translation along the axis y_r) (Tora, 2008).

The upper platform mechanism (also referred to as the Sarrus mechanism) is placed upon platform 6. It consists of 6 boards (four of them are shown in Fig. 3) connected in twos by revolving pairs whilst the neighbouring boards are positioned transverse one to another. This mechanism, therefore, has 1 degree of mobility and the cab moves perpendicularly to platform 6. It is set in motion by the cylinder hitched in the joints F and H.

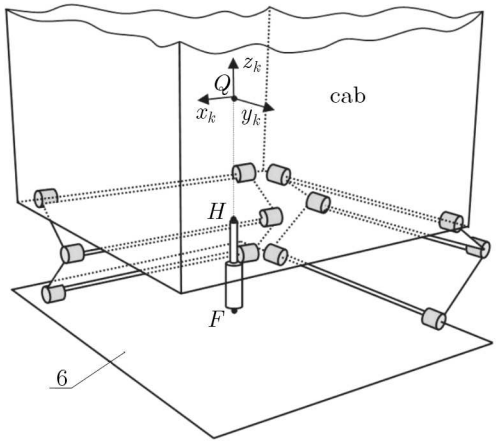

Fig. 3. Upper platform mechanism elevating the cab in the vertical direction

3. Coordinate systems

Four systems of coordinates are considered. The first immobile system $x_g y_g z_g$ is associated with the distance travelled by the machine. The z_g-axis is parallel to the vector of acceleration of gravity $\boldsymbol{g}$. In this system, we define the function of road profile on which the machine travels. The system $x_r y_r z_r$ is mobile and is associated with the machine frame. The centre point of the frame is at the point O (Fig. 1, Fig. 2), the versors of axes are: $\boldsymbol{i}_1^x$, $\boldsymbol{i}_1^y$, $\boldsymbol{i}_1^z$. Another mobile system $x_m y_m z_m$ is in-between the $x_g y_g z_g$ and $x_r y_r z_r$. The origin of the system $x_m y_m z_m$ is at the point O and the z_m-axis is parallel to the acceleration of gravity vector $\boldsymbol{g}$ whilst the axes z_m, x_m and x_r are coplanar. The last condition satisfies the requirement that the direction of the gravity force $\boldsymbol{g}$ in the system $x_r y_r z_r$ should be taken into consideration. The coordinate

system $x_m y_m z_m$ should be utilised to show the versor of the gravity force: ${}^m\boldsymbol{i}_g = [0, 0, -1]$, which shall be expressed in the system $x_r y_r z_r$ using the transition matrix ${}^r_m\mathbf{R}$ from the coordinate system $x_m y_m z_m$ to $x_r y_r z_r$

$$\boldsymbol{i}_g = {}^r_m\mathbf{R}\ {}^m\boldsymbol{i}_g \tag{3.1}$$

The direction of the gravity force is of primary importance for two reasons: firstly – the active suspension ought to position the cab along $\boldsymbol{i}_g$, secondly – the actuator load is imposed by the gravity force acting upon the cab. The fourth coordinate system $x_k y_k z_k$ is associated with the cab, the versors of its axes are: $\boldsymbol{i}_6^x$, $\boldsymbol{i}_6^y$, $\boldsymbol{i}_6^z$. The origin of this coordinate system Q is in the centre of mass of the cab. While modelling the operation of the active suspension, the rotation matrix ${}^r_k\mathbf{R}$ has to be defined, from $x_k y_k z_k$ (the cab) to $x_r y_r z_r$ (the frame). The elements of the matrix ${}^r_k\mathbf{R}$ are obtained basing on versors in the system associated with the cab expressed in that associated with the frame. Accordingly, we get

$${}^r_k\mathbf{R} = \begin{bmatrix} \boldsymbol{i}_6^x \boldsymbol{i}_1^x & 0 & \boldsymbol{i}_6^z \boldsymbol{i}_1^x \\ \boldsymbol{i}_6^x \boldsymbol{i}_1^y & \boldsymbol{i}_6^y \boldsymbol{i}_1^y & \boldsymbol{i}_6^z \boldsymbol{i}_1^y \\ \boldsymbol{i}_6^x \boldsymbol{i}_1^z & \boldsymbol{i}_6^y \boldsymbol{i}_1^z & \boldsymbol{i}_6^z \boldsymbol{i}_1^z \end{bmatrix} \tag{3.2}$$

The second element in the first row is equal to zero because $\boldsymbol{i}_6^y \perp \boldsymbol{i}_1^x$ (Fig. 2).

4. Kinematics of the actuating mechanism

Basic quantities used in kinematic equations are versors associated with particular links of the mechanism. The versors are expressed in the system associated with the frame. This study is limited in scope, so the kinematics of link position for the given mechanism involves only solving the inverse problem where the lengths of cylinders s_4 and s_5 have to be found for the predetermined horizontal position of platform 6. The versor of the cab vertical axis $\boldsymbol{i}_6^z = [i_{6x}^z, i_{6y}^z, i_{6z}^z]^\top$ should have the opposite direction to that of the gravity versor

$$\boldsymbol{i}_6^z = -\boldsymbol{i}_g \tag{4.1}$$

The coordinates of versors of the mechanism links: $\boldsymbol{i}_6^y = [0, i_{6y}^y, i_{6z}^y]^\top$, $\boldsymbol{i}_2 = [0, i_{2y}, i_{2z}]^\top$, $\boldsymbol{i}_3 = [0, i_{3y}, i_{3z}]^\top$, $\boldsymbol{i}_4 = [0, i_{4y}, i_{4z}]^\top$, $\boldsymbol{i}_5 = [i_{5x}, i_{5y}, i_{5z}]^\top$ and instantaneous lengths of the cylinders s_4 and s_5 are obtained by solving equations that are derived recalling (Fig. 2):

— orthogonality of versors of platform 6

$$\boldsymbol{i}_6^y \boldsymbol{i}_6^z = 0 \tag{4.2}$$

— triangle COD

$$l_{CO}\boldsymbol{i}_1^y + l_2\boldsymbol{i}_2 = s_4\boldsymbol{i}_4 \tag{4.3}$$

— quadrilateral ODEB

$$l_2\boldsymbol{i}_2 + l_6\boldsymbol{i}_6^y + l_3\boldsymbol{i}_3 = l_1\boldsymbol{i}_1^y \tag{4.4}$$

— polygon KAGFDO

$$l_{KA}\boldsymbol{i}_1^y + s_5\boldsymbol{i}_5 + l_{GF}\boldsymbol{i}_6^x = l_{KO}\boldsymbol{i}_1^x + l_2\boldsymbol{i}_2 + \frac{1}{2}l_6\boldsymbol{i}_6^y \tag{4.5}$$

Equations (4.2) and (4.3)-(4.5) projected onto the directions of the coordinate system associated with the frame axes $x_r y_r z_r$ can be easily transformed into the system of polynomial equations of the second degree. In this case, an explicit solution is found though an arbitrary decision is still required and one solution has to be selected which meets the requirements imposed by the configuration of the mechanism. For the upper mechanism, the equation is used that defines the position of point O in the coordinate system associated with the frame $x_r y_r z_r$

$$\boldsymbol{l}_{OQ} = l_2\boldsymbol{i}_2 + \frac{1}{2}l_6\boldsymbol{i}_6^y + (s_6 + l_{HQ})\boldsymbol{i}_6^z \tag{4.6}$$

The quantity s_6 present in (4.6) is obtained using the integral of the rate of change of the cylinder length (during the vertical motion of the cab) v_6. That is why we can eliminate cumbersome field measurements of the frame position with respect to the immobile system $x_g y_g z_g$.

As platform 6 rotating round frame 1 might move around the axes of joints defined by the versors $\boldsymbol{i}_1^x$ and $\boldsymbol{i}_6^y$, we can easily predict the form of the equation of the angular velocity vector of platform 6

$$\boldsymbol{\omega}_6 = \boldsymbol{\omega}_1 + \omega_{61p}\boldsymbol{i}_1^x + \omega_{61b}\boldsymbol{i}_6^y \tag{4.7}$$

where: ω_{61p}, ω_{61b} – velocity component of the platform 6 with respect to the frame 1 in the direction $\boldsymbol{i}_1^x$ and $\boldsymbol{i}_1^y$, respectively.

The vectors of angular velocity of links 2, 3 and 4 are represented as the sum of angular velocity vector of frame 1 and the product of the directional vector $\boldsymbol{i}_1^x$ and the modulus of relative velocity ω_{j1}

$$\boldsymbol{\omega}_j = \boldsymbol{\omega}_1 + \omega_{j1}\boldsymbol{i}_1^x \qquad j = 2, 3, 4 \tag{4.8}$$

Derivatives of equations (4.3)-(4.5) are utilised to find ω_{61p} and ω_{61b}

$$\begin{aligned} &l_{CO}\boldsymbol{\omega}_1 \times \boldsymbol{i}_1^y + l_2\boldsymbol{\omega}_2 \times \boldsymbol{i}_2 = v_4\boldsymbol{i}_4 + s_4\boldsymbol{\omega}_4 \times \boldsymbol{i}_4 \\ &l_2\boldsymbol{\omega}_2 \times \boldsymbol{i}_2 + l_6\boldsymbol{\omega}_6 \times \boldsymbol{i}_6^y + l_3\boldsymbol{\omega}_3 \times \boldsymbol{i}_3 = l_1\boldsymbol{\omega}_1 \times \boldsymbol{i}_1^y \\ &l_{KA}\boldsymbol{\omega}_1 \times \boldsymbol{i}_1^y + s_5\boldsymbol{\omega}_5 \times \boldsymbol{i}_5 + v_5\boldsymbol{i}_5 + l_{GF}\boldsymbol{\omega}_6 \times \boldsymbol{i}_6^x = \\ &\quad = l_{KO}\boldsymbol{\omega}_1 \times \boldsymbol{i}_1^x + l_2\boldsymbol{\omega}_2 \times \boldsymbol{i}_2 + \frac{1}{2}l_6\boldsymbol{\omega}_6 \times \boldsymbol{i}_6^y \end{aligned} \tag{4.9}$$

Obtaining the dot product of $\boldsymbol{i}_4$ and Eq. $(4.9)_1$, and substituting (4.8) into $(4.9)_1$ yields

$$\omega_{21} = \frac{v_4}{l_2\boldsymbol{i}_1^x \times \boldsymbol{i}_2\boldsymbol{i}_4} = \frac{v_4}{r_1} \tag{4.10}$$

Obtaining the dot product of $\boldsymbol{i}_3$ and Eq. $(4.9)_2$, and substituting (4.7), (4.8) and (4.10) into $(4.9)_2$ yields

$$\omega_{61p} = -\frac{v_4}{\frac{r_1 l_6(\boldsymbol{i}_1^x \times \boldsymbol{i}_6^y \boldsymbol{i}_3)}{l_2 \boldsymbol{i}_1^x \times \boldsymbol{i}_2 \boldsymbol{i}_3}} = \frac{v_4}{r_3} \tag{4.11}$$

Obtaining the dot product of $\boldsymbol{i}_5$ and Eq. $(4.9)_3$, and substituting (4.7), (4.8), (4.10), (4.11) into $(4.9)_3$ yields

$$\omega_{61b} = \frac{v_4}{\frac{l_{GF}\boldsymbol{i}_6^z \boldsymbol{i}_5}{\boldsymbol{i}_1^x \times \left[\frac{(l_{GF}\boldsymbol{i}_6^x - \frac{1}{2}l_6\boldsymbol{i}_6^y)}{r_3} - \frac{l_2\boldsymbol{i}_2}{r_1}\right]\boldsymbol{i}_5}} + \frac{v_5}{l_{GF}\boldsymbol{i}_6^z\boldsymbol{i}_5} = \frac{v_4}{r_4} + \frac{v_5}{r_5} \tag{4.12}$$

Finally, the vector of angular velocity of the cab becomes

$$\boldsymbol{\omega}_6 = \boldsymbol{\omega}_1 + v_4\Big(\frac{\boldsymbol{i}_1^x}{r_3} + \frac{\boldsymbol{i}_6^y}{r_4}\Big) + v_5\frac{\boldsymbol{i}_6^y}{r_5} = \boldsymbol{\omega}_1 + v_4\boldsymbol{E}_4 + v_5\boldsymbol{E}_5 \tag{4.13}$$

Linear velocity of the point Q derived from Eq. (4.6) is

$$\boldsymbol{v}_Q = \boldsymbol{v}_O + l_2\boldsymbol{\omega}_2 \times \boldsymbol{i}_2 + \boldsymbol{\omega}_6 \times \Big(\frac{1}{2}l_6\boldsymbol{i}_6^y + (s_6 + l_{HQ})\boldsymbol{i}_6^z\Big) + v_6\boldsymbol{i}_6^z \tag{4.14}$$

Substituting Eq (4.7), (4.8), (4.11), (4.12) into Eq (4.14) yields

$$\boldsymbol{v}_Q = \boldsymbol{v}_O + \boldsymbol{\omega}_1 \times \boldsymbol{l}_{OQ} + v_4\boldsymbol{C}_4 + v_5\boldsymbol{C}_5 + v_6\boldsymbol{C}_6 \tag{4.15}$$

where

$$\boldsymbol{C}_4 = \Big(\frac{l_2}{r_1}\boldsymbol{i}_1^x \times \boldsymbol{i}_2 + \boldsymbol{E}_4 \times \boldsymbol{l}_{DQ}\Big) \qquad \boldsymbol{C}_5 = \boldsymbol{E}_5 \times \boldsymbol{l}_{DQ} \qquad \boldsymbol{C}_6 = \boldsymbol{i}_6^z$$

Equations of angular velocity of platform 6 and cab (4.13) and velocities of the point Q are now used to find the angular and linear acceleration

$$\begin{aligned}\boldsymbol{\varepsilon}_6 &= \boldsymbol{\varepsilon}_1 + a_4\boldsymbol{E}_4 + a_5\boldsymbol{E}_5 + \boldsymbol{\varepsilon}_\Omega \\ \boldsymbol{a}_Q &= \boldsymbol{a}_O + \boldsymbol{\varepsilon}_1 \times \boldsymbol{l}_{OQ} + a_4\boldsymbol{C}_4 + a_5\boldsymbol{C}_5 + a_6\boldsymbol{C}_6 + \boldsymbol{a}_\Omega\end{aligned} \tag{4.16}$$

where

$$\begin{aligned}\boldsymbol{\varepsilon}_\Omega &= v_4\frac{d}{dt}\boldsymbol{E}_4 + v_5\frac{d}{dt}\boldsymbol{E}_5 \\ \boldsymbol{a}_\Omega &= v_4\frac{d}{dt}\boldsymbol{C}_4 + v_5\frac{d}{dt}\boldsymbol{C}_5 + v_6\frac{d}{dt}\boldsymbol{C}_6 + \boldsymbol{\omega}_1 \times \frac{d}{dt}\boldsymbol{l}_{OQ}\end{aligned}$$

5. Conditions of motion of the actuating mechanism

The active suspension mechanism of the cab controls its angular velocity in the directions $\boldsymbol{i}_1^x$ and $\boldsymbol{i}_6^y$, where the following conditions can be imposed upon angular velocity of the cab

$$\boldsymbol{\omega}_6\boldsymbol{i}_1^x = 0 \qquad \boldsymbol{\omega}_6\boldsymbol{i}_6^y = 0 \tag{5.1}$$

Conditions (5.1) in conjunction with (4.13) yield instantaneous velocities in the cylinders of the lower mechanism

$$v_4 = -r_3\boldsymbol{\omega}_1\boldsymbol{i}_1^x \qquad v_5 = -r_5\boldsymbol{\omega}_1\Big(\boldsymbol{i}_6^y - \boldsymbol{i}_1^x\frac{r_3}{r_4}\Big) \tag{5.2}$$

When the cylinders move at the speed given by (5.2), the cab shall perform rotary motion only in the direction $\boldsymbol{i}_1^x \times \boldsymbol{i}_6^y$. The cylinder s6 controls the linear motion of point Q along the direction of the versor $\boldsymbol{i}_6^z$. Such velocity v_6 can be induced that the point Q should be immobile in the direction of the z_m axis

$$\boldsymbol{v}_Q\boldsymbol{i}_g = 0 \tag{5.3}$$

Substituting (5.2) into (4.15) yields

$$v_6 = -\frac{\Big(\boldsymbol{v}_O + \boldsymbol{\omega}_1 \times \boldsymbol{l}_{OQ} + v_4\boldsymbol{C}_4 + v_5\boldsymbol{C}_5\Big)\boldsymbol{i}_g}{\boldsymbol{C}_6\boldsymbol{i}_g} \tag{5.4}$$

Conditions (5.2) imposed upon the angular velocity of platform 6, when differentiated, are transformed into acceleration formulas

$$\boldsymbol{\varepsilon}_6\boldsymbol{i}_1^x + \boldsymbol{\omega}_6(\boldsymbol{\omega}_1 \times \boldsymbol{i}_1^x) = 0 \qquad \boldsymbol{\varepsilon}_6\boldsymbol{i}_6^y = 0 \tag{5.5}$$

Recalling $(4.16)_1$, we get

$$\begin{aligned} &a_4\boldsymbol{E}_4\boldsymbol{i}_1^x + a_5\boldsymbol{E}_5\boldsymbol{i}_1^x + (\boldsymbol{\varepsilon}_1 + \boldsymbol{\varepsilon}_\Omega)\boldsymbol{i}_1^x + (v_4\boldsymbol{E}_4 + v_5\boldsymbol{E}_5)(\boldsymbol{\omega}_1 \times \boldsymbol{i}_1^x) = 0 \\ &a_4\boldsymbol{E}_4\boldsymbol{i}_6^y + a_5\boldsymbol{E}_5\boldsymbol{i}_6^y + (\boldsymbol{\varepsilon}_1 + \boldsymbol{\varepsilon}_\Omega)\boldsymbol{i}_6^y = 0 \end{aligned} \tag{5.6}$$

On solving the linear system of equations we get accelerations of cylinders 4 and 5. Similarly, differentiating (5.3) and recalling $d\boldsymbol{i}_g/dt = -\boldsymbol{\omega}_1 \times \boldsymbol{i}_g$ and $(4.16)_2$ yields the formula expressing the acceleration of the cylinder responsible for the cab motion in the vertical direction

$$a_6 = \frac{\boldsymbol{v}_Q(\boldsymbol{\omega}_1 \times \boldsymbol{i}_g) - (\boldsymbol{a}_O + \boldsymbol{\varepsilon}_1 \times \boldsymbol{l}_{OQ} + a_4\boldsymbol{C}_4 + a_5\boldsymbol{C}_5 + \boldsymbol{a}_\Omega)\boldsymbol{i}_g}{\boldsymbol{C}_6\boldsymbol{i}_g} \tag{5.7}$$

6. Dynamics of the actuating mechanism

The dynamic model assumes that the mechanism contains holonomic two-sided constraints. Of major interest are gravity forces, inertia and the driving force whilst link deformations and drive elasticity are neglected. The frame mass is assumed to be much larger than that of the cab whilst the cab mass is decidedly larger than the masses of the actuating mechanism links. The relationship between the masses reveals that in the dynamic model the excitation inducing motion of the cab can be treated as kinematic and that the forces of gravity and inertia of the mechanism links can be neglected (Frączek *et al.*, 2008). The inertia force and moment are obtained from Newton's and Euler's equations (Morecki *et al.*, 2002)

$$\boldsymbol{P}_b = -m_k\boldsymbol{a}_Q \qquad \boldsymbol{M}_b = -(\mathbf{I}_k\boldsymbol{\varepsilon}_6 + \widetilde{\boldsymbol{\omega}}_6\mathbf{I}_k\boldsymbol{\omega}_6) \tag{6.1}$$

The mass moment of the cab inertia $\mathbf{I}_k$ expressed in the coordinate system associated with the frame is given as

$$\mathbf{I}_k = {}^r_k\mathbf{R}\ {}^k\mathbf{I}_k\ {}^r_k\mathbf{R}^\top \tag{6.2}$$

where ${}^k\mathbf{I}_k$ is the moment of the cab inertia in the system associated with the cab.

For the considered mechanism, the equation of instantaneous power balance can be formulated, where the sum of power expended by the drives and power associated with the force and moment of inertia and the gravity of the cab should be equal to zero

$$\boldsymbol{Q}_{dr}^\top\boldsymbol{v} + m_k(\boldsymbol{g} - \boldsymbol{a}_Q)^\top(\boldsymbol{v}_Q - \boldsymbol{v}_O - \boldsymbol{\omega}_1 \times \boldsymbol{l}_{OQ}) + (-\mathbf{I}_k\boldsymbol{\varepsilon}_6 - \widetilde{\boldsymbol{\omega}}_6\mathbf{I}_k\boldsymbol{\omega}_6)^\top(\boldsymbol{\omega}_6 - \boldsymbol{\omega}_1) = 0 \tag{6.3}$$

where

$$\boldsymbol{Q}_{dr} = [Q_{dr4}, Q_{dr5}, Q_{dr6}]^{\top} \qquad \boldsymbol{v} = [v_4, v_5, v_6]^{\top}$$

Recalling (4.13) and (4.15) with respect to (6.3), we get

$$\boldsymbol{Q}_{dr}^{\top}\boldsymbol{v} + m_k(\boldsymbol{g} - \boldsymbol{a}_Q)^{\top}\boldsymbol{C}\boldsymbol{v} + (-\mathbf{I}_k\boldsymbol{\varepsilon}_6 - \widetilde{\boldsymbol{\omega}}_6\mathbf{I}_k\boldsymbol{\omega}_6)^{\top}\boldsymbol{E}\boldsymbol{v} = 0 \tag{6.4}$$

where

$$\boldsymbol{C} = [\boldsymbol{C}_4, \boldsymbol{C}_5, \boldsymbol{C}_6]^{\top} \qquad \boldsymbol{E} = [\boldsymbol{E}_4, \boldsymbol{E}_5, \mathbf{0}]^{\top}$$

It follows from (6.4) that

$$\boldsymbol{Q}_{dr} = m_k\boldsymbol{C}^{\top}(\boldsymbol{a}_Q - \boldsymbol{g}) + \boldsymbol{E}^{\top}(\mathbf{I}_k\boldsymbol{\varepsilon}_6 + \widetilde{\boldsymbol{\omega}}_6\mathbf{I}_k\boldsymbol{\omega}_6) \tag{6.5}$$

7. Simulation of performance of the active suspension system of the cab

Equations of kinematics and dynamics of the mechanism of the cab active suspension become the starting point for simulations, assuming the kinematic model of excitations acting upon the frame as shown in Fig. 4. The frame is represented by a front bridge (P_P, P_L), a longitudinal frame (P, T) and point O at which the active suspension is connected. The rear bridge (T_L, T_P) is connected to the longitudinal frame via a rotating joint. The direction of the longitudinal axis is represented by the versor ${}^m\boldsymbol{i}_1^x$ and that of the front bridge is defined by the versor ${}^m\boldsymbol{i}_1^y$. It is assumed that velocity components along the axis x_g of extreme points of the front and rear bridge should be constant and equal to v_p whilst velocity components in the direction y_g should equal zero. Velocity components in the direction z_g are associated with the machine's travel on curvilinear profiles

$$\begin{aligned} z_{T_P} &= z_{max}\sin\Big(2\pi\frac{v_{P_x}t}{L}\Big) & z_{P_P} &= z_{max}\sin\Big(2\pi\frac{v_{Px}t + d^*}{L}\Big) \\ z_{T_L} &= z_{max}\sin\Big(2\pi\frac{v_{Px}t}{L} + \varphi\Big) & z_{P_P} &= z_{max}\sin\Big(2\pi\frac{v_{Px}t + d^*}{L} + \varphi\Big) \end{aligned} \tag{7.1}$$

where L is the wavelength, z_{max} – amplitude, w – bridge width, d – distance between the front and rear bridge, φ – phase shift angle of the road profile between the left- and right-hand side, $d^* = d\,{}^m\boldsymbol{i}_1^x\,{}^m\boldsymbol{i}_x \approx d$.

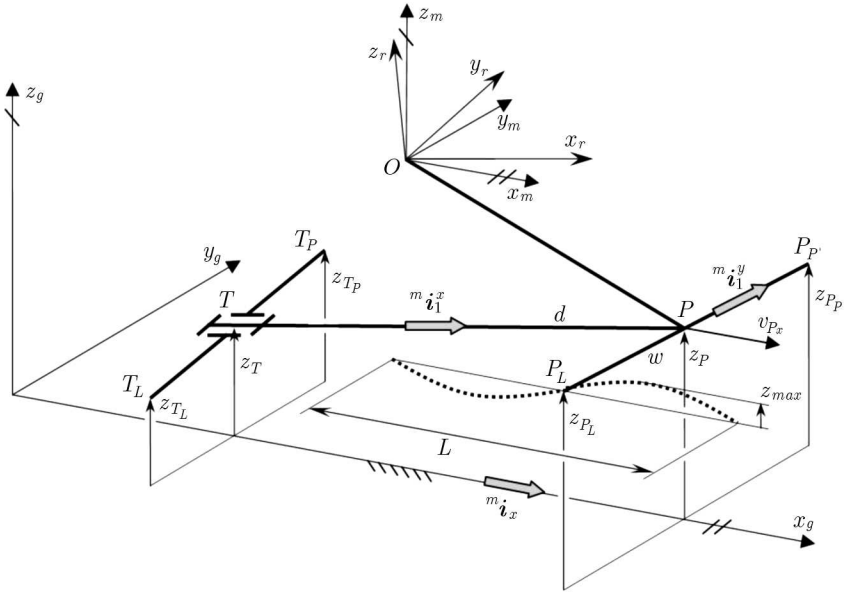

Fig. 4. Model of kinematic excitation inducing motion of the frame

The versor coordinates of the frame expressed in the $x_m y_m z_m$ coordinate system are

$$
{}^m\boldsymbol{i}_1^x = \left[\sqrt{1-\left(\frac{z_P - z_T}{d}\right)^2}, 0, \frac{z_P - z_T}{d}\right]
$$

$$
{}^m\boldsymbol{i}_1^y = \left[0, \sqrt{1-\left(\frac{z_{P_P} - z_{P_L}}{w}\right)^2}, \frac{z_{P_P} - z_{P_L}}{w}\right] \qquad {}^m\boldsymbol{i}_1^z = {}^m\boldsymbol{i}_1^x \times {}^m\boldsymbol{i}_1^y \tag{7.2}
$$

where: $z_P = (z_{P_P} + z_{P_L})/2,\ z_T = (z_{T_P} + z_{T_L})/2$.

The versor coordinates of the coordinate system associated with the frame yield a matrix

$$
{}^r_m\mathbf{R} = \begin{bmatrix} {}^m i_{1x}^x & 0 & {}^m i_{1z}^x \\ 0 & {}^m i_{1y}^y & {}^m i_{1z}^y \\ {}^m i_{1x}^z & {}^m i_{1y}^z & {}^m i_{1z}^z \end{bmatrix} \tag{7.3}
$$

The angular velocity of the frame in the coordinate system $x_m y_m z_m$ is given as

$$
{}^m\boldsymbol{\omega}_1 = [{}^m\omega_{1x}, {}^m\omega_{1y}, 0] \tag{7.4}
$$

The ngular velocity components are derived from the system of equations

$$
\dot{z}_P - \dot{z}_T = d({}^m\boldsymbol{\omega}_1 \times {}^m\boldsymbol{i}_1^x)^z \qquad \dot{z}_{P_P} - \dot{z}_{P_L} = w({}^m\boldsymbol{\omega}_1 \times {}^m\boldsymbol{i}_1^y)^z \tag{7.5}
$$

Accordingly, the desired angular velocity components of the frame are

$$ {}^{m}\omega_{1x} = \frac{\dot{z}_{P_P} - \dot{z}_{P_L}}{w\ {}^{m}i_{1y}^{y}} \qquad {}^{m}\omega_{1y} = -\frac{\dot{z}_P - \dot{z}_T}{d\ {}^{m}i_{1x}^{x}} \tag{7.6} $$

The parameters required for simulations, i.e. angular velocity of the frame and linear velocity of the point O should be determined in the coordinate system associated with the frame

$$ \boldsymbol{\omega}_1 = {}_{m}^{r}\mathbf{R}\ {}^{m}\boldsymbol{\omega}_1 \qquad v_O = {}_{m}^{r}\mathbf{R}\ {}^{m}\boldsymbol{v}_P + \boldsymbol{\omega}_1 \times \boldsymbol{r}_{PO} \tag{7.7} $$

where: ${}^{m}\boldsymbol{v}_P = [\dot{z}_P, 0, v_{Px}]$, $\boldsymbol{r}_{PO}$ is a known, constant vector defined in the coordinate system of the frame.

Simulations are performed for various values of the velocity v_{Px}. Its maximum value is associated with the fact that the wheels must remain in contact with the road. Comparing the acceleration of gravity to the maximal acceleration of an arbitrary extreme point on the frame bridges, we get

$$ v_{Px\ max} = \frac{L}{2\pi}\sqrt{\frac{g}{z_{max}}} \tag{7.8} $$

To evaluate the effects of the active suspension on linear acceleration of the point Q of the cab, we use the acceleration reduction factor λ relating to effective accelerations in the selected direction $(x_m, y_m)(\lambda_z = 0)$, the active suspension system being on and off

$$ \lambda = \sqrt{\frac{\int_0^{t_k} a_Q^2\ dt}{\int_0^{t_k} a_{Qout}^2\ dt}} \tag{7.9} $$

Evaluation of the system performance takes into account the energy "costs" required to power-supply the active suspension. In the present study, this aspect of the system operation is addressed by considering the energy expended to support the work of the cab active suspension related to the energy difference between the vibrating motion of the cab in the on and off states

$$ \bigwedge_{N_4,N_5,N_6,N_{out},N_{on}>0} \qquad \tau = \frac{\int_0^{t_k}(N_4 + N_5 + N_6)\ dt}{\int_0^{t_k} N_{out}\ dt - \int_0^{t_k} N_{on}\ dt} \tag{7.10} $$

where: $N_{out} = m_k \boldsymbol{v}_{Qout}(-\boldsymbol{a}_{Qout}+\boldsymbol{g})+\boldsymbol{\omega}_1(-\mathbf{I}_k\boldsymbol{\varepsilon}_1-\widetilde{\boldsymbol{\omega}}_1\mathbf{I}_k\boldsymbol{\omega}_1)$ is the power expended by the drive during the cab motion with the active suspension in the off state, $\boldsymbol{v}_{Qout}$, $\boldsymbol{a}_{Qout}$ – velocity and acceleration of the cab centre of gravity with the active suspension in the off state. $N_{on} = m_k \boldsymbol{v}_Q(-\boldsymbol{a}_Q+\boldsymbol{g})+\boldsymbol{\omega}_6(-\mathbf{I}_k\boldsymbol{\varepsilon}_6-\widetilde{\boldsymbol{\omega}}_6\mathbf{I}_k\boldsymbol{\omega}_6)$ is the power expended by the drive during cab motion with the active suspension in the on state, $N_4 = Q_{dr4}v_4$, $N_5 = Q_{dr5}v_5$, $N_6 = Q_{dr6}v_6$ are power ratings of individual drives while the active suspension system is on.

Simulation data were gathered for the road profile defined by the parameters: $L = 2\,\mathrm{m}$, $z_{max} = 0.1\,\mathrm{m}$, $\varphi = 1.57\,\mathrm{rad}$. The maximum velocity derived from (7.8) is equal to: $v_{max} = 3.15\,\mathrm{m/s}$. Simulation time is $t_k = 120\,\mathrm{s}$. The computer model of the cab yields the cab mass ($m_k = 469\,\mathrm{kg}$) and the matrix of inertia moment values of the cab expressed in the coordinate system associated with the cab

$$ {}^{k}\mathbf{I}_k = \begin{bmatrix} 133.05 & -0.28 & -21.47 \\ -0.28 & 197.37 & 0.29 \\ -21.47 & 0.29 & 148.04 \end{bmatrix} \ \mathrm{kg\,m^2} $$

The simulation results are shown in the form of graphs and all relevant quantities are expressed in function of the quotient of velocity in the horizontal motion and its maximum value: $k_x = v_{Px}/v_{Px\,max}$.

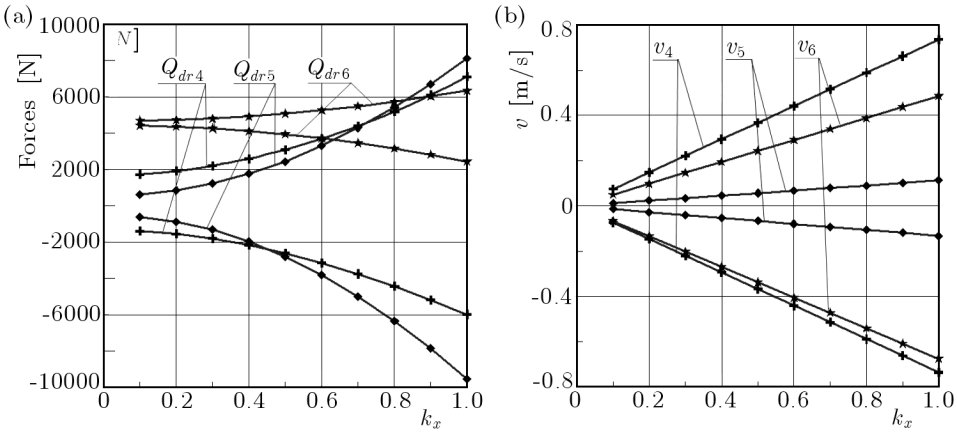

Fig. 5. Maximal and minimal forces (a) and velocity (b) in the cylinders

The maximum and minimum values of drive loading and velocity (Fig. 5) do not exceed the admissible levels for typical hydraulic drives. The average loading of the drive in the vertical motion (Fig. 5a) corresponds to the force of gravity acting on the cab. Larger power consumption by cylinder 4 (Fig. 6)

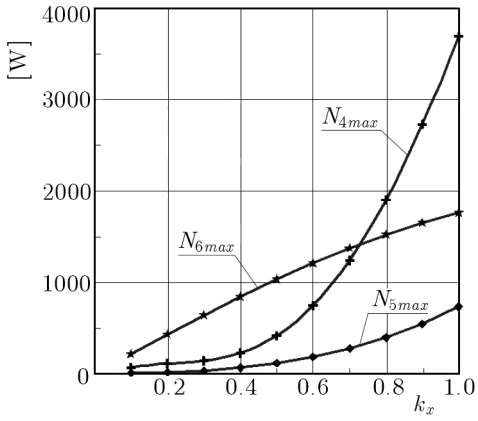

Fig. 6. Maximum power developed in the cylinders

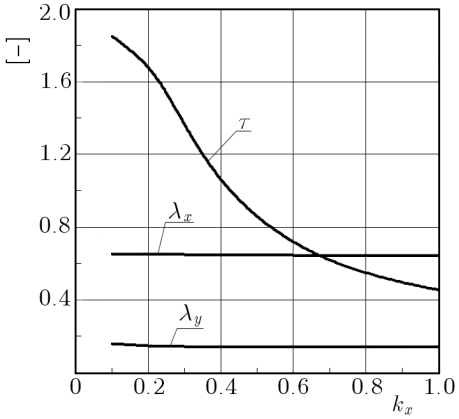

Fig. 7. Vibration reduction factor during cab motion in the direction (x, y). Energy consumption factor

is attributable to the fact that it has to handle two DOFs. Although the active suspension mechanism is not intended for vibration reduction in the direction coinciding with ride of the cab, vibration damping still occurs $\lambda_x \approx 0.65$, see Fig. 7, being the side effect of vibration reduction in the rotating motion of the cab around $\boldsymbol{i}_6^y$ $(5.1)_2$. Control of velocity of cylinder 4 is the consequence of reduction of rotation around $\boldsymbol{i}_1^x$ $(5.1)_1$, yet the proper size of links of the suspension mechanisms ensures considerable vibration reduction in the direction transverse to the truck ride $\lambda_y \approx 0.14$, Fig. 7. The active suspension system, when in service, reduces acceleration of the cab, which in turn lowers the loading due to inertia. Thus, energy required by the driving

system to move the cab is lower, too, which is corroborated by the energy consumption pattern τ (Fig. 7). For $k_x > 0.42$, the total energy expended by the driving system and the active suspension to move the cab is less than energy required to move the cab whilst the active suspension mechanism is off, $\tau < 1$.

8. Conclusions

The results have to be treated as approximate as in the underlying model the drives shall instantaneously implement the computed velocity and the motion of the machine frame is well known beforehand. In practical applications, however, the system for motion control will be of key importance and the important measurable excitation comes in the shape of the frame motion. That would require a control strategy to compensate for the effects of these disturbances. In order that the system for measuring the frame motion should be autonomous, the system of acceleration sensors can be applied. To determine instantaneous velocities of the drives (5.2) and (5.4), it is required that linear and angular velocity of the frame motion should be known. That poses certain problems, however, as constant has to be precisely determined and the precision of acceleration signal integration has to be reliably established. Cylinders 4 and 5, maintaining the cab in the vertical position, operate without the risk of exceeding the motion range. Cylinder 6, responsible for the cab motion in the vertical direction, might quickly reach its critical length while the cab begins its ride upwards or downwards. The method of finding the length of cylinder 6 should be such that its motion range should not be exceeded. Condition $(5.1)_1$ relating to the rotary motion of the cab (rotation round $\boldsymbol{i}_1^x$) might be replaced by the condition formulated for the linear motion of the cab: $\boldsymbol{v}_Q \boldsymbol{i}_1^y = 0$. It is reasonable to expect that energy consumption by cylinder 4 should be smaller. The axis of the load band of cylinder 6 is shifted upwards by the value of the statistical gravity load (Fig. 5a). This load, and hence power demand, might be reduced when the upper mechanism is provided with an incorporated system of relieving springs, reducing the loading of drive 6 by the cab weight. The major step in the calculation procedure involves finding the transition matrix from the $x_m y_m z_m$ to $x_r y_r z_r$ systems – ${}^r_m\mathbf{R}$. In this study, the matrix is derived basing on the model of the road and the machine suspension. In practical applications, the matrix elements should be determined from measurements of two angles of the frame deflection from the vertical direction.

References

1. Anthonis J., De Temmerman J., Deprez K., Ramon H., 2004, Conceptual cab suspension system for a self-propelled agricultural machine. Part 1: Development of a linear mathematical model, *Biosystems Engineering*, **89**, 4, 409-416

2. Anthonis J., De Temmerman J., Deprez K., Ramon H., 2005, Conceptual cab suspension system for a self-propelled agricultural machine. Part 2: Operator comfort optimisation, *Biosystems Engineering*, **90**, 3, 271-278

3. Benamar F., Grand Ch., Plumet F., 2010, Motion kinematics analysis of wheeled-legged rover over 3D surface with posture adaptation, *Mechanism and Machine Theory*, **45**, 477-495

4. Cardou P., Angeles J., 2008, Angular-velocity estimation from the centripetal component of the rigid-body acceleration field, *Advances in Robot Kinematics: Analysis and Design*, Springer Science + Busines Media B.V., 354-360

5. Frączek J., Wojtyra M., Davliakos I., Papadopoulos E., 2008, Simulational study of a hydraulicly driven parallel manipulator control system, *Journal of KONES Powertrain and Transport*, **15**, 1, 51-67

6. Michałowski S., 2001, *Redukowanie wibracji w maszynach roboczych ciężkich*, PIT, Kraków

7. Morecki A., Knapczyk J., Kędzior K., 2002, *Teoria Mechanizmów i manipulatorów*, WNT, Warszawa

8. Nakano K., Suda Y., Nakadai S., Tsunashima H., Washizu T., 1999, Self-powered active control applied to a truck cab suspension, *JSAE*, **20**, 511-516

9. Solarz W., Tora G., 2003, Mechanizm platformowy o 5 stopniach swobody w układzie aktywnej stabilizacji położenia kabiny maszyny roboczej, *Posiedzenie Sekcji Podstaw Technologii Komitetu Budowy Maszyn PAN*, Nowy Sącz, 85-91

10. Tora G., 2002, Applications of platform mechanisms with 6 DOFs in active vibration control systems, *The Archive of Mechanic Engineering*, **XLIX**, 2, 181-193

11. Tora G., 2008, Mechanizm platformowy w układzie aktywnej redukcji drgań, *Materiały XXI Ogólnopolskiej Konferencji Naukowo-Dydaktycznej Teorii Maszyn i Mechanizmów*, Bielsko-Biała, 357-366

Analiza pracy aktywnego zawieszenia kabiny maszyny roboczej

Streszczenie

Artykuł stanowi etap prac dotyczących aktywnego zawieszenia kabiny maszyny roboczej, służącego do redukcji drgań niskoczęstotliwościowych o dużej amplitudzie. Zawieszenie składa się z dwóch mechanizmów platformowych umieszczonych jeden na drugim. Dolny mechanizm jest odpowiedzialny za utrzymanie kabiny w pionie. Górny mechanizm odpowiada za ruch kabiny w kierunku pionowym. Do opisu ruchu wykorzystano wersory związane z ogniwami mechanizmu. Wyprowadzono zależności na chwilowe prędkości napędów, powodujących redukcję drgań kabiny maszyny w wybranych stopniach swobody. Przedstawiono sposób obliczania obciążeń napędów aktywnego zawieszenia kabiny dla znanego ruchu ramy maszyny. Na podstawie matematycznego modelu wykonano symulacje pracy zawieszenia.

Manuscript received October 27, 2009; accepted for print February 26, 2010